



UvA-DARE (Digital Academic Repository)

Scaphoid fractures: anatomy, diagnosis and treatment

Buijze, G.A.

Publication date
2012

[Link to publication](#)

Citation for published version (APA):

Buijze, G. A. (2012). *Scaphoid fractures: anatomy, diagnosis and treatment*. [Thesis, fully internal, Universiteit van Amsterdam].

General rights

It is not permitted to download or to forward/distribute the text or part of it without the consent of the author(s) and/or copyright holder(s), other than for strictly personal, individual use, unless the work is under an open content license (like Creative Commons).

Disclaimer/Complaints regulations

If you believe that digital publication of certain material infringes any of your rights or (privacy) interests, please let the Library know, stating your reasons. In case of a legitimate complaint, the Library will make the material inaccessible and/or remove it from the website. Please Ask the Library: <https://uba.uva.nl/en/contact>, or a letter to: Library of the University of Amsterdam, Secretariat, P.O. Box 19185, 1000 GD Amsterdam, The Netherlands. You will be contacted as soon as possible.

Chapter

3

Osseous and ligamentous scaphoid anatomy: Part II Evaluation of ligament morphology using three-dimensional anatomical imaging

Buijze GA, Dvinskikh NA, Strackee SD, Streekstra GJ,
Blankevoort L



Abstract

Purpose There are many controversies in the literature regarding the morphology of the scaphoid ligaments. The aim of this study was to provide a more accurate description by quantitatively describing the 3-dimensional, geometrical aspects of the scaphoid ligaments and their attachments, using cryomicrotome images of cadaveric wrists.

Methods Eight fresh-frozen human cadaver wrists were examined with computed tomography (CT) and an imaging cryomicrotome. A series of 2-dimensional cryoimages created a 3-dimensional anatomical data set of each test specimen. Detection of ligaments and their surface areas was performed by manually marking the course and attachment points for each ligament, using dedicated visualization software. The 3-dimensional bone surfaces were segmented from the acquired CT images and incorporated in the 3-dimensional anatomical data set of the same anatomical specimen to facilitate the detection procedure. The results of the morphological parameters and attachment areas of the scaphoid ligaments are described 3-dimensionally.

Results The mean size of the whole scaphoid surface was $1503 \pm 17 \text{ mm}^2$, and the mean size of all ligament attachments on the scaphoid was $131 \pm 14 \text{ mm}^2$; thus, ligament attachments consist of $9\% \pm 0.9\%$ of the total scaphoid surface area. Based on the data, a 3-dimensional representation of the wrist was created to present the scaphoid ligament attachment areas and paths. The dorsal intercarpal ligament had the most individual variability between specimens in attachments.

Conclusions The quantitative results were almost completely consistent with the findings of previous reports. The only inconsistency in ligament morphology regarded the scaphocapitate ligament, which in this study was found to be the thickest ligament attached to the scaphoid.

Clinical relevance The results of this study improve our knowledge of scaphoid ligament anatomy, as they corroborate previous findings. This is important for carpal surgery and will pave the way to a better understanding of the biomechanics involved in destabilization of wrist fractures.



Introduction

The ligaments attached to the scaphoid play a critical role in wrist kinematics and carpal stability.^{1,2} When the scaphoid is fractured, its role is accentuated, as the ligaments affect the stability of the fracture fragments. It is, therefore, important for the assessment and repair of scaphoid fractures and/or ligament injuries to have an accurate anatomical knowledge of the ligament attachments and morphology. The exact anatomy is necessary to distinguish potentially stable from potentially unstable fractures, thus finding the relationship between pathological biomechanics and ligament anatomy. The accurate description of ligament attachments and bone shape of individual scaphoids is required for reliable biomechanical analysis of scaphoid fractures and for carpal surgery.

There are many controversies in the literature regarding the morphology of the scaphoid ligaments, as reported in part one of this study.³ This heterogeneity in quantifications and descriptions of wrist ligaments is most likely due to the difficulty of accurately studying such complex soft tissue anatomy macroscopically when dissecting cadavers. Controversy of ligament descriptions is a typical issue in other joints as well.^{4,5} Typically, dissections, arthroscopy, and magnetic resonance imaging have been used to describe wrist ligaments. The imaging cryomicrotome system offers a reliable solution to the problem of limited macroscopic visualization of dissections. Cryomicrotome sections provide detailed 3-dimensional images of joint structures.

The cryomicrotome system has axial and lateral resolution of about 0.15 mm,⁶ allowing 3-dimensional imaging with voxel size in the order of hundredths of millimeters. Such an accurate quantitative detection of cartilage surfaces and ligament geometry of the wrist using this methodology has recently been reported and has been reproduced in the current study.⁷

The primary aim of this study was to provide both a more accurate and a quantitative description of the 3-dimensional geometrical aspects of the scaphoid ligaments and their attachment areas by using 3-dimensional anatomical images of cadaveric wrists. The secondary aim was to verify the attachment of ligaments whose descriptions in the literature are most consistent.

Materials and Methods

Eight fresh-frozen human cadaver wrists with a mean age of 81 years (range, 72 to 85 y) were examined with computed tomography (CT) and an imaging cryomicrotome. The medical history and CT scans of the donors were examined to ensure that there was no history of previous wrist injury or pathology. Segmentation of the carpals, radius, and ulna was performed from the CT image, using a region-growing algorithm

as previously described.⁸ Starting from a seed point, a weighted average was calculated within a small sphere (radius, 1.5 voxel). Whenever this averaged gray value was higher than a predefined gray level, this voxel was classified as bone and assigned to the bone region in the process of growing. This segmentation result comprises at least the hard bone structure at the rim of the bone but does not always comprise the complete inner bone structure. Therefore, a binary closing operation is used to close the outline of the carpal.

Cryosectioning was performed using a cryostatic microtome system.^{6,7} The stack of consecutive 2-dimensional images builds up a 3-dimensional image of each test specimen. Before imaging the cadaver specimen, the cryomicrotome system was calibrated by using a calibration object so that the pixel size of the digital image was $100 \times 100 \mu\text{m}^2$. The resulting 3-dimensional voxel size was $100 \times 100 \times 100 \mu\text{m}^3$. Carpals and cartilage were imaged by applying white light. The ligaments and tendons were imaged by using the autofluorescence properties of collagen type I that is present in these anatomical structures, as the cryomicrotome imaging system allows for simultaneous acquisition in white light and fluorescence mode.^{6,7} The imaging system also detects collagen present in the bone. However, the 3-dimensional imaging system made it possible to distinguish between collagen in bone and outside bone based on location and appearance because the ligaments appear in fiber structures.

One observer performed ligament detection by manually marking the outer contours (representing the ligament borders) and the attachment points for each ligament, using the landmark function in the visualization software, Amira 4.1 (Konrad-Zuse-Zentrum für Informationstechnik, Berlin, Germany). Four contour curves were detected, representing the width and thickness of the ligament bundle along its path. To detect the 2 contour curves characterizing ligament thickness (Fig. 1A), an arbitrarily oriented plane was sought in which the full length of the ligament was visible. Subsequently, a curved plane was fitted through the centerline between the 2 contour curves orthogonal to the first plane. This curved plane also followed the ligament path from origin to insertion and was used to detect the 2 contour curves characterizing the width of the ligament bundle (Fig. 1B).

The 4 contour curves served as guides for the detection of the ligament bundle attachments. In addition, the bone surfaces segmented from the CT scans were incorporated in the 3-dimensional anatomical images to facilitate the marking of the ligament attachments to the bone surface. The voxel size of the CT scan was resampled to the voxel size of the cryomicrotome image. Subsequently, the CT image was aligned and fused with the cryomicrotome image.

The ligament attachment areas were detected and marked by scrolling through planes parallel to the direction of ligament bundles at the insertion sites. Each detected area was represented by a 3-dimensional point cloud, a collection of points in space that (in this study) all followed a curved surface pattern representing a ligament or

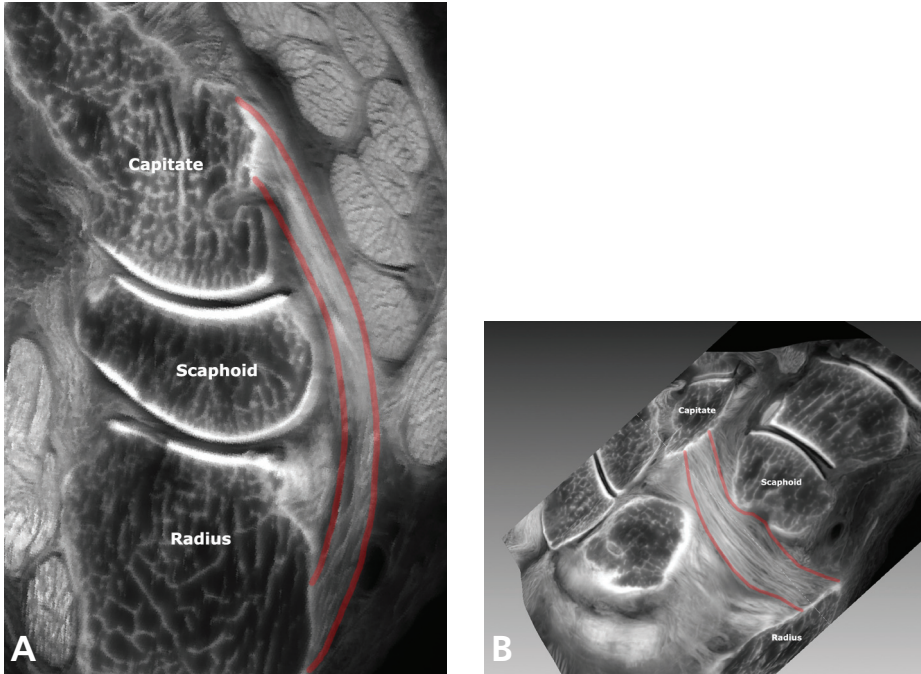


Figure 1: Cryomicrotome image of a right wrist showing **A** an oblique sagittal plane through the estimated center of the radioscapohcapitate ligament and **B** a curved, coronal surface fitted through this curved ligament, orthogonal to the oblique sagittal plane, to visualize its entire course from origin to insertion. The red lines indicate the margins of the ligament and indicate its thickness and width. Several ligament bundles deviate from the main ligament, directing radially to its attachment on the scaphoid.

bone structure. Using Amira 4.1 software, the acquired point clouds were used for the estimation of ligament attachment areas, and bone surface areas were calculated based on the bone surfaces segmented from CT scans.

Ligament lengths were calculated in Matlab R2007b (Mathworks, Natick, MA), using the average of the lengths of the 4 curves representing a ligament bundle. Ligament widths and thicknesses were estimated at a position in the middle of the ligament trajectory. Ligaments were described according to the nomenclature of Berger.⁹ Statistical analysis of the differences (within the group) in measurements of length, width, and thickness of the scaphoid ligaments at various attachment sites was performed with a paired *t*-test, with the level of significance set at $P < .05$.

Results

The results of the morphological parameters of the ligaments that attached to the scaphoid are given in Table 1. The attachment areas of the ligaments are given in Table 2, and the attachment areas as a percentage of the total scaphoid bone

Table 1. Morphological Parameters of Scaphoid Ligament Morphology						
	Length (mm)		Width (mm)		Thickness (mm)	
	Mean	SD	Mean	SD	Mean	SD
Volar ligaments						
Radioscaphocapitate	29,8	1,7	5,1	0,8	1,4	0,3
Scaphocapitate	14,0	1,2	6,7	0,9	2,2	0,4
Scaphotrapezoidal	8,8	2,6	1,9	0,6	0,9	0,3
Scaphotrapezial	7,2	1,0	6,7	1,0	1,2	0,2
Transverse carpal	30,1	3,8	14,6	4,9	1,5	0,3
Radioscapholunate	8,3	1,1	2,5	0,4	1,2	0,2
Dorsal ligaments						
Dorsal intercarpal	32,6	2,3	6,3	1,5	1,2	0,2
Scapholunate interosseous ligaments						
Volar scapholunate interosseous	4,0	0,8	5,8	1,0	1,3	0,3
Proximal scapholunate interosseous	5,4	1,5	11,9	1,5	1,4	0,4
Dorsal scapholunate interosseous	3,7	0,7	7,4	0,9	1,6	0,3

surface (attachment area of each ligament as part of the total osseous surface of the scaphoid) and the total ligament attachment area (attachment area of each ligament as part of the total ligament attachment surface of the scaphoid) are given in Table 3. For visualization purposes, a 3-dimensional representation of a wrist (that was most representative of the group) was created to present the scaphoid ligament attachment areas and paths from a volar and dorsal view (Figs. 2A, 2B).

Volar Ligaments

Two ligaments ran from the radius to the scaphoid: the radioscapholunate ligament and the radioscaphocapitate ligament. The radioscapholunate ligament was one of the smallest extrinsic ligaments that attached to the scaphoid and had comparable attachment surface areas on the lunate and scaphoid. The radioscaphocapitate ligament mainly ran from the volar side of the radial styloid to the volar central part of the capitate head, with more than three-quarters of the fibers bypassing the scaphoid waist. In all 8 wrists, less than one-quarter of the ligament bundle deviated from the main ligament to a relatively much smaller attachment (approximately one-quarter of the size of the capitate attachment area) on the proximal edge of the scaphoid tubercle (Fig. 1B). Adjacent to the radioscaphocapitate ligament was the scaphocapitate ligament, which attached to the volar capitate head, just radial of the radioscaphocapitate ligament. The scaphocapitate ligament was the thickest scaphoid ligament (mean, 2.2 ± 0.4 mm) and had the largest attachment surface area (mean,



Table 2. Scaphoid Ligament Attachments and Surface Areas

		Area (mm ²)	
		Mean	SD
Volar ligaments			
Radioscaphocapitate	Radius	15,7	5,1
	Scaphoid	3,2	1,1
	Capitate	13,3	3,2
Scaphocapitate	Scaphoid	51,9	9,3
	Capitate	16,6	4,3
Scaphotrapezoidal	Scaphoid	3,6	3,3
	Trapezoid	3,2	3,4
Scaphotrapezial	Scaphoid	11,3	4,7
	Trapezium	12,3	3,4
Transverse carpal	Scaphoid	5,9	1,7
	Trapezium	30,9	9,2
	Pisiform	7,8	2,9
	Hamatum	30,2	5,8
Radioscapholunate	Radius	4,3	2,5
	Scaphoid	1,7	0,7
	Lunate	2,4	0,7
Dorsal ligaments			
Dorsal intercarpal	Triquetrum	10,2	3,5
	Scaphoid prox	7,3	4,3
	Scaphoid waist	6,4	2,3
	Lunatum	3,9	0,4
	Trapezoid	4,5	2,3
	Trapezium	3,6	-
Scapholunate interosseous ligaments			
Volar scapholunate interosseous	Scaphoid	8,2	2,6
	Lunate	7,9	3,3
Proximal scapholunate interosseous	Scaphoid	21,0	5,7
	Lunate	25,5	9,2
Dorsal scapholunate interosseous	Scaphoid	10,2	3,0
	Lunate	9,4	3,2

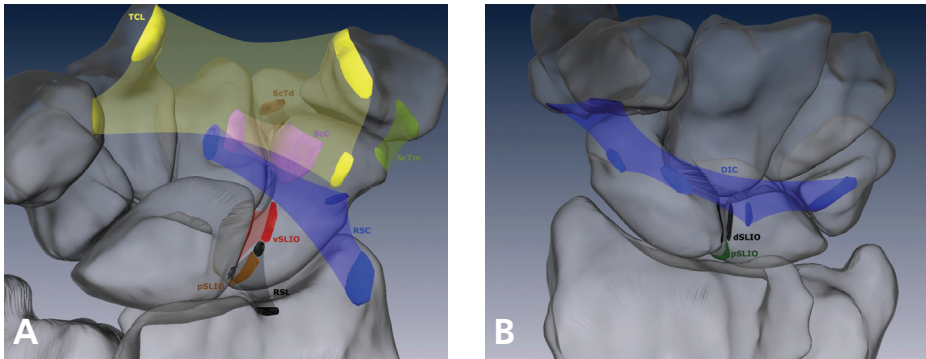


Figure 2: A Volar and B dorsal views of the 3-dimensional representation of the wrist, showing the scaphoid ligaments and the attachments. TCL, transverse carpal ligament; ScTd, scaphotrapezoidal ligament; ScC, scaphocapitate ligament; ScTm, scaphotrapezium ligament; vSLIO, volar scapholunate interosseous ligament; RSC, radioscaphocapitate ligament; pSLIO, proximal scapholunate interosseous ligament; RSL, radioscapholunate ligament; DIC, dorsal intercarpal ligament; dSLIO, dorsal scapholunate interosseous ligament.

51.9 ± 9.3 mm²) of all scaphoid ligaments. Its attachment to the scaphoid covered almost the entire ulnar part of the scaphoid tubercle and represented nearly 40% of the total surface area of all scaphoid attachments. The attachment on the capitate was much more compact (mean, 16.6 ± 4.3 mm²) and consisted of less than one-third of the attachment on the scaphoid.

The scaphotrapezoidal ligament originated directly distal to the scaphocapitate ligament and represented the narrowest and thinnest scaphoid ligament and inserted on the volar proximal lip of the trapezoid. The attachments on the scaphoid (mean, 3.6 ± 3.3 mm²) were comparable in size to those of the trapezoid (mean, 3.2 ± 3.4 mm²). The scaphotrapezium ligament, consisting of a single bundle, originated on the radial distal part of the scaphoid tubercle, just lateral to the flexor carpi radialis tendon sheath. In all wrists, the attachment on the scaphoid (mean, 11.3 mm² ± 4.7 mm²) appeared to be slightly narrower (although not smaller) than that of the trapezium (mean, 12.3 mm² ± 3.4 mm²), which gave the ligament a trapezoid-like shape (or V shape).

The transverse carpal ligament mainly ran between the hook of hamate and the volar ridge of the trapezium, but it also had attachments on the pisiform and scaphoid. The attachment on the scaphoid was the smallest (mean, 5.9 mm² ± 1.7 mm²) of all 4 attachments, with means ranging from 7.8 mm² on the pisiform to 30.9 mm² on the trapezium. The transverse carpal ligament was the widest ligament that had an attachment to the scaphoid.

All the volar ligaments described were found to have an attachment on the scaphoid in all 8 of the imaged wrists.



Table 3. Surface Areas of Scaphoid Ligament Attachments as Percentage of Total Surface Area

	Area/scaphoid surface (%) [*]		Area/total ligament surface (%) [†]	
	Mean	SD	Mean	SD
Volar ligaments				
Radioscaphocapitate	0,2	0,7	2,4	0,9
Scaphocapitate	3,5	5,3	39,8	7,1
Scaphotrapezoidal	0,2	1,9	2,7	2,5
Scaphotrapezial	0,8	2,7	8,6	3,6
Transverse carpal ligament	0,4	1,0	4,5	1,3
Radioscapholunate	0,1	0,4	1,3	0,6
Volar total	5,2	0,8	59,3	8,7
Dorsal ligaments				
Dorsal intercarpal				
Proximal scaphoid	0,5	2,4	5,6	3,3
Waist scaphoid	0,4	1,3	4,9	1,8
Dorsal total	0,9	0,3	10,5	3,7
Scapholunate interosseous ligaments				
Volar scapholunate interosseous	0,5	1,5	6,3	2,0
Proximal scapholunate interosseous	1,4	3,2	16,1	4,4
Dorsal scapholunate interosseous	0,7	1,7	7,8	2,3
Scapholunate interosseous total	2,6	0,5	30,2	5,3
Total ligament surface	8,7	0,9	-	-

^{*}Attachment area of each ligament as part of the total osseous surface of the scaphoid.

[†]Attachment area of each ligament as part of the total ligament attachment surface of the scaphoid.

Dorsal Ligaments

On the dorsal side of the wrist, only one ligament attached to the scaphoid: the dorsal intercarpal ligament. The dorsal intercarpal ligament was the longest ligament attaching to the scaphoid (mean, 32.6 ± 2.3 mm). It originated from the dorsoradial side of the triquetrum and inserted in both the proximal and waist areas of the dorsoradial ridge of the scaphoid in all imaged wrists. In some of the wrists, there were additional attachments to the lunate (2/8), the trapezoid (6/8), and the trapezium (1/8). No other ligament was found to attach to the scaphoid; in particular, the radial collateral ligament bypassed the scaphoid radiodorsally, and none of its bundles inserted in the scaphoid in any of the 8 wrists.

Scapholunate interosseous ligament

The scapholunate interosseous ligament was a single C-shaped ligament, consisting of 3 parts: a volar, dorsal, and proximal part. The 3 parts could not be clearly distinguished by an interruption of the continuity of the bundles but were rather defined for the reason of comparison, based on their anatomical location as well as the horizontal or vertical direction of the bundle's course between the scaphoid and lunate.¹⁰ The volar scapholunate interosseous and dorsal scapholunate interosseous ligaments were comparable in length, but the width (7.4 ± 0.9 mm) and thickness (1.6 ± 0.3 mm) of the dorsal part were slightly and significantly larger than the width (5.8 ± 1.0 mm) and thickness (1.3 ± 0.3 mm) of the volar part ($P < .05$). The proximal scapholunate interosseous ligament was both the longest and widest portion of the ligament. It originated on the ulnar edge of the scaphoid and inserted in the proximal edge of the lunate, with a double curve in the coronal plane, thus forming an S shape (Fig. 3).

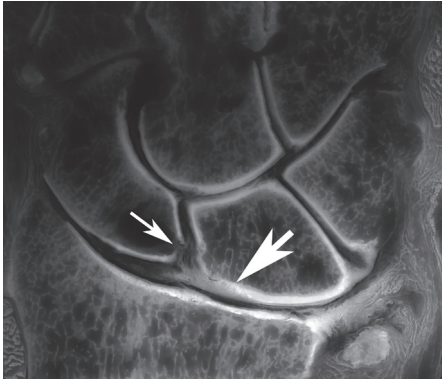


Figure 3: Cryomicrotome image in the coronal plane of a right wrist showing a cross-section of the proximal scapholunate interosseous ligament. The origin of the ligament is located on the ulnar edge of the scaphoid (thin arrow), and the insertion is located on the proximal edge of the lunate (thick arrow).

Discussion

The results of this study present an overview of the detailed 3-dimensional quantification of all ligaments that attach to the scaphoid, including variability between individual specimens. Nagao et al described the ligament attachments of the lunate in 3 dimensions, with details of locations and attachment areas.¹⁰ This technique provides extensive details of the ligaments that attach to the lunate, the distal carpal row, and the proximal ends of the metacarpals.^{10–14} This study provides similarly detailed 3-dimensional descriptions for the scaphoid ligaments.

Some of the ligament morphology and attachment areas reported in our study were described previously, based on specimen dissections.^{10,13,15} Our quantitative data were almost completely within the range of the 95% confidence interval of the previously reported ligament dimensions. The only inconsistency in ligament morphology regarded the scaphocapitate ligament, which, in this study, was the thickest ligament



attached to the scaphoid. The mean thickness dimension (2.2 ± 0.4 mm) was notably larger than that reported by Nanno et al (0.9 ± 0.2 mm).¹³ Similar to their findings, we found a large disparity between the attachment areas of the scaphocapitate ligament on the scaphoid and the capitate, but the disparity in our study was not as great.

The radioscaphocapitate ligament has previously been described on magnetic resonance images,¹⁶ as well as in 65 cadaveric wrists.¹⁵ The results from the latter study were comparable to those found in our study. Similar to the findings of Berger and Landsmeer, we found that the bulk of the radioscaphocapitate ligament takes an arcuate course around the volar scaphoid waist, with only a few fibers inserting on the proximal surface of the scaphoid tubercle.¹⁷ However, in contrast to their findings, the bulk of fibers seemed to insert mostly on the capitate (Figs. 1A, 1B) and did not seem to interdigitate predominantly with fibers arching toward the ulna and triquetrum. A radial collateral ligament inserting into the scaphoid was not found. Instead we found a capsular-like structure that bypassed the scaphoid radiodorsally along its surface, with its fibers directed distally. No volar¹⁶ or dorsal¹⁸⁻²¹ radioscaphoid ligament was detected.

The volar scaphotriquetral ligament, as described by Sennwald et al²² and Smith,¹⁶ was not detected as a separate ligament in our study. We found these bundles (that correspond to this ligament) to interdigitate with the volar arcuate ligament (consisting of the interdigitating radioscaphocapitate, scaphocapitate, triquetrocipitate, and ulnocapitate ligaments) and could not confirm the absence of an attachment to the capitate.

The scaphotrapezial and scaphotrapezoidal ligaments found in our study were not fully consistent with most previous anatomical descriptions, most of which did not report a scaphotrapezoidal ligament.^{9,13,23-26} The dimensions in our study are comparable to those of Nanno et al, except for the finding that there was no ulnar scaphotrapezial ligament bundle in any of the specimens.¹³ The thin scaphotrapezoidal ligament described in the current study, similar to Berger's description,⁹ would most likely be part of a thin scaphotrapezial-trapezoidal capsule, which forms the floor of the flexor carpi radialis tendon sheath.

Our findings of the transverse carpal ligament, originating from the hook of the hamate and pisiform and inserting onto the entire volar trapezial ridge and the scaphoid, are consistent with previous findings.^{13,24,27-29} Although its attachment on the scaphoid is the smallest of all 4 bony attachments, disruption of the ligament (eg, after carpal tunnel release surgery) has been shown to notably affect scaphoid kinematics.^{30,31} However, a clinical significance has not been proven.

The dorsal intercarpal ligament, originating on the dorsal radial surface of the triquetrum, was found in all our specimens to insert in both the proximal and the mid-waist areas of the dorsoradial ridge of the scaphoid. In 7 of 8 specimens, the dorsal intercarpal ligament continued distally to either the dorsoradial rim of the trapezium or

the trapezoid. The additional attachment to the lunate was found in 2 of 8 specimens, which is somewhat different from the findings of Nagao et al¹⁰ and Viegas,³² in which the authors found a lunate attachment in 75% or more of specimens.

Regarding the scapholunate interosseous ligament, our findings were mostly consistent with previous reports.^{10,33-37} One notable finding is that the attachment of the proximal scapholunate interosseous ligament on the lunate was more proximal and ulnar than previously described, which gives the ligament an S shape with 2 opposite curves in the coronal plane (Fig. 3). This might explain why the proximal scapholunate interosseous ligament was slightly longer than the volar and dorsal parts.

The results of this study should be interpreted in light of several limitations. First, considering the fact that only 8 wrists were investigated in this study, no conclusions should be drawn with regard to the variability between individual specimens in ligament morphology (such as for the dorsal intercarpal ligament) other than the fact that there was substantial variability between individuals. The variation in patterns of the dorsal intercarpal ligament have previously been well described.^{32,38} Second, unlike dissections and arthroscopy, cryomicrotome imaging is a static imaging method and does not allow for ligament tensioning as a way to verify attachments. We relied solely on interpretation of images in an unlimited amount and unrestricted shapes of planes.

The major strength of this study lies in its advanced imaging methodology that allows for high accuracy. Previous dissections, which used a digitizer, had an accuracy of 0.23 mm for the digitizer and an additional accuracy limitation related to the observer's detection.¹⁰⁻¹⁴ Our imaging method has an accuracy of 0.1 mm.

The morphology of the scaphoid ligaments is complex and variable between individual wrists. The results of this study enhance our understanding of the anatomy of the wrist ligaments, a controversial topic that is evolving as visualization methods improve.

References

1. Tang JB, Ryu J, Han JS, Omokawa S, Kish V, Wearden S. Biomechanical changes of the wrist flexor and extensor tendons following loss of scaphoid integrity. *J Orthop Res* 1997;15:69–75.
2. Short WH, Werner FW, Green JK, Masaoka S. Biomechanical evaluation of ligamentous stabilizers of the scaphoid and lunate. *J Hand Surg* 2002;27A:991–1002.
3. Buijze GA, Lozano-Calderon SA, Strackee SD, Blankevoort L, Jupiter JB. Osseous and ligamentous scaphoid anatomy: part I. A systematic literature review highlighting controversies. *J Hand Surg* 2011;36A:1926–1935.
4. Amis AA, Firer P, Mountney J, Senavongse W, Thomas NP. Anatomy and biomechanics of the medial patellofemoral ligament. *Knee* 2003;10:215–220.
5. Rucco V, Basadonna PT, Gasparini D. Anatomy of the iliolumbar ligament: a review of its anatomy and a magnetic resonance study. *Am J Phys Med Rehabil* 1996;75:451–455.
6. Rolf MP, ter Wee R, van Leeuwen TG, Spaan JA, Streekstra GJ. Diameter measurement from images of fluorescent cylinders embedded in tissue. *Med Biol Eng Comput* 2008;46:589–596.
7. Dvinskikh NA, Blankevoort L, Foumani M, Spaan JA, Streekstra GJ. Quantitative detection of cartilage surfaces and ligament geometry of the wrist using an imaging cryomicrotome system. *J Biomech* 2010;43:1007–1010.
8. Carelsen B, Jonges R, Strackee SD, Maas M, van Kemenade P, Grimbergen CA, et al. Detection of in vivo dynamic 3-D motion patterns in the wrist joint. *IEEE Trans Biomed Eng* 2009;56:1236–1244.
9. Berger RA. The ligaments of the wrist. A current overview of anatomy with considerations of their potential functions. *Hand Clin* 1997;13:63–82.
10. Nagao S, Patterson RM, Buford WL Jr, Andersen CR, Shah MA, Viegas SF. Three-dimensional description of ligamentous attachments around the lunate. *J Hand Surg* 2005;30A:685–692.
11. Nanno M, Patterson RM, Viegas SF. Three-dimensional imaging of the carpal ligaments. *Hand Clin* 2006;22:399–412.
12. Nanno M, Buford WL, Jr., Patterson RM, Andersen CR, Viegas SF. Three-dimensional analysis of the ligamentous attachments of the first carpometacarpal joint. *J Hand Surg* 2006;31A:1160–1170.
13. Nanno M, Buford WL Jr, Patterson RM, Andersen CR, Viegas SF. Three-dimensional analysis of the ligamentous attachments of the second through fifth carpometacarpal joints. *Clin Anat* 2007;20:530–544.
14. Kijima Y, Viegas SF. Wrist anatomy and biomechanics. *J Hand Surg* 2009;34A:1555–1563.
15. Wozasek GE, Laske H. The ligaments of the scaphoid bone. *Handchir Mikrochir Plast Chir* 1991;23:18–22.
16. Smith DK. Volar carpal ligaments of the wrist: normal appearance on multiplanar reconstructions of three-dimensional Fourier transform MR imaging. *Am J Roentgenol* 1993;161:353–357.
17. Berger RA, Landsmeer JM. The palmar radiocarpal ligaments: a study of adult and fetal human wrist joints. *J Hand Surg* 1990;15A:847–854.
18. Taleisnik J. The bones of the wrist. In: Taleisnik J, ed. *The wrist*. New York: Churchill Livingstone, 1985:1–12.
19. Lipscomb PR. The wrist and hand. In: Hollinshead WH, ed. *Anatomy for surgeons*. New York: Harper & Row, 1969:455–459.
20. Schmidt H, Lanz U. *Chirurgische anatomie der hand*. 1st ed. Stuttgart: Hippokrates Verlag, 1992:46–80.



21. Fahrer M. Introduction to anatomy of the wrist. In: Tubiana R, ed. *The hand*. Philadelphia: WB Saunders, 1981:130–135.
22. Sennwald GR, Zdravkovic V, Oberlin C. The anatomy of the palmar scaphotriquetral ligament. *J Bone Joint Surg* 1994;76B:147–149.
23. Taleisnik J. The ligaments of the wrist. *J Hand Surg* 1976;1:110–118.
24. Bettinger PC, Linscheid RL, Berger RA, Cooney WP 3rd, An KN. An anatomic study of the stabilizing ligaments of the trapezium and trapeziometacarpal joint. *J Hand Surg* 1999;24A:786–798.
25. Moritomo H, Viegas SF, Nakamura K, Dasilva MF, Patterson RM. The scaphotrapezio-trapezoidal joint. Part 1: An anatomic and radiographic study. *J Hand Surg* 2000;25A:899–910.
26. Drenwiany JJ, Palmer AK, Flatt AE. The scaphotrapezial ligament complex: an anatomic and biomechanical study. *J Hand Surg* 1985;10A:492–498.
27. Stecco C, Macchi V, Lancerotto L, Tiengo C, Porzionato A, De Caro R. Comparison of transverse carpal ligament and flexor retinaculum terminology for the wrist. *J Hand Surg* 2010;35A:746–753.
28. Nigro RO. Anatomy of the flexor retinaculum of the wrist and the flexor carpi radialis tunnel. *Hand Clin* 2001;17:61–64.
29. Pacek CA, Chakan M, Goitz RJ, Kaufmann RA, Li ZM. Morphological analysis of the transverse carpal ligament. *Hand (N Y)* 2010;5:135–140.
30. Ishiko T, Puttitz CM, Lotz JC, Diao E. Scaphoid kinematic behavior after division of the transverse carpal ligament. *J Hand Surg* 2003;28A:267–271.
31. Tengrootenhuysen M, van Riet R, Pimontel P, Bortier H, Van Glabbeek F. The role of the transverse carpal ligament in carpal stability: an in vitro study. *Acta Orthop Belg* 2009;75:467–471.
32. Viegas SF, Yamaguchi S, Boyd NL, Patterson RM. The dorsal ligaments of the wrist: anatomy, mechanical properties, and function. *J Hand Surg* 1999;24A:456–468.
33. Berger RA. The gross and histologic anatomy of the scapholunate interosseous ligament. *J Hand Surg* 1996;21A:170–178.
34. Berger RA, Blair WF, Crowninshield RD, Flatt AE. The scapholunate ligament. *J Hand Surg* 1982;7A:87–91.
35. Berger RA, Imeada T, Berglund L, An KN. Constraint and material properties of the subregions of the scapholunate interosseous ligament. *J Hand Surg* 1999;24A:953–962.
36. Berger RA. The anatomy of the scaphoid. *Hand Clin* 2001;17:525–532.
37. Sokolow C, Saffar P. Anatomy and histology of the scapholunate ligament. *Hand Clin* 2001;17:77–81.
38. Smith DK. Dorsal carpal ligaments of the wrist: normal appearance on multiplanar reconstructions of three-dimensional Fourier transform MR imaging. *Am J Roentgenol* 1993;161:119–125.